

Aggravated inflammation and increased expression of cysteinyl leukotriene receptors in the brain after focal cerebral ischemia in AQP4-deficient mice

Wen-Zhen Shi¹, Chun-Zhen Zhao¹, Bing Zhao¹, Qiao-Juan Shi¹, Li-Hui Zhang², Yan-Fang Wang², San-Hua Fang¹, Yun-Bi Lu¹, Wei-Ping Zhang¹, Er-Qing Wei¹

¹*Institute of Neuroscience and Department of Pharmacology, School of Medicine, Zhejiang University, Hangzhou 310058, China*

²*Hangzhou Key Laboratory of Neurobiology and Department of Pharmacology, School of Basic Medicine, Hangzhou Normal University, Hangzhou 310036, China*

© Shanghai Institutes for Biological Sciences, CAS and Springer-Verlag Berlin Heidelberg 2012

Abstract: Objective Aquaporin-4 (AQP4), the main water channel protein in the brain, plays a critical role in water homeostasis and brain edema. Here, we investigated its role in the inflammatory responses after focal cerebral ischemia. **Methods** In AQP4-knockout (KO) and wild-type mice, focal cerebral ischemia was induced by 30 min of middle cerebral arterial occlusion (MCAO). Ischemic neuronal injury and cellular inflammatory responses, as well as the expression and localization of cysteinyl leukotriene CysLT₂ and CysLT₁ receptors, were determined at 24 and 72 h after MCAO. **Results** AQP4-KO mice showed more neuronal loss, more severe microglial activation and neutrophil infiltration, but less astrocyte proliferation in the brain after MCAO than wild-type mice. In addition, the protein levels of both CysLT₁ and CysLT₂ receptors were up-regulated in the ischemic brain, and the up-regulation was more pronounced in AQP4-KO mice. The CysLT₁ and CysLT₂ receptors were primarily localized in neurons, microglia and neutrophils; those localized in microglia and neutrophils were enhanced in AQP4-KO mice. **Conclusion** AQP4 may play an inhibitory role in post-ischemic inflammation.

Keywords: aquaporin 4; gene deficiency; inflammation; cysteinyl leukotriene receptor; microglia; astrocyte; focal cerebral ischemia

1 Introduction

Aquaporin-4 (AQP4), the water channel protein mainly expressed in the brain^[1,2], is primarily localized in astrocytes^[3] and plays a critical role in water homeostasis and edema in the brain^[2]. From the investigations of AQP4-

deficient mice, AQP4 has been found to promote cytotoxic edema but attenuate vasogenic edema after brain injury^[4]. In addition, AQP4 is a regulator in processes unrelated to edema, such as astrocyte migration and glial scar formation^[4,5], astrocytic Ca²⁺ signaling^[6], and striatal neurotransmitter release^[7].

With regard to the role of AQP4 in brain inflammation, AQP4 expression is associated with inflammation in multiple sclerosis, human immunodeficiency virus encephalitis or progressive multifocal leukoencephalopa-

Corresponding author: Er-Qing Wei
Tel: +86-571-88208224; Fax: +86-571-88208022
E-mail: weiq2006@zju.edu.cn
Article ID: 1673-7067(2012)06-0680-13
Received date: 2012-03-10; Accepted date: 2012-04-06

thy^[8], experimental autoimmune encephalomyelitis^[9,10], neuromyelitis optica (NMO)^[11,12], hemorrhage^[13] or after intracerebral injection of lipopolysaccharide^[14] or lyssolecithin^[15]. Especially in NMO, an inflammatory autoimmune demyelinating disease, AQP4 is a specific target because an IgG1 autoantibody (NMO-IgG) against AQP4 has been identified in the sera of a significant number of NMO patients^[11,12]. NMO-IgG down-regulates AQP4 in astrocytes, leads to the accumulation of toxic molecules and astrocyte dysfunction, and thereby results in demyelination and aggravates edema^[12,16,17]. In these changes, NMO-IgG-induced dysfunction of astrocytes is the determining event because activated astrocytes limit the development of inflammation^[12,18]. AQP4 is also important in astrocyte proliferation, one of the responses to inflammation, because AQP4 knockdown using siRNA inhibits astrocyte proliferation^[19].

However, the role of AQP4 in post-ischemic inflammation is poorly understood. Post-ischemic inflammation involves the accumulation of inflammatory cells (resident microglia and blood-derived leukocytes) and the induction of pro-inflammatory molecules^[20-22]. As inflammatory mediators, cysteinyl leukotrienes (CysLTs) through activating their receptors (CysLT₁ and CysLT₂) evoke post-ischemic inflammation^[23-26]. CysLT₁ and CysLT₂ receptors are up-regulated and localized in activated microglia and proliferated astrocytes in the ischemic brain in rats^[24,26]. The CysLT₁ receptor regulates ischemia-induced astrocyte proliferation and glial scar formation as well^[27,28]. However, how AQP4 deficiency impacts the expression and localization of CysLT₁ and CysLT₂ receptors remains unknown.

In the present study, we investigated the inflammatory responses, i.e. accumulation of microglia and blood-derived leukocytes, and the expression of inflammation-associated CysLT₁ and CysLT₂ receptors, in AQP4-knockout (KO) mice.

2 Materials and methods

2.1 Animals AQP4-KO mice and matched CD1 littermates were kindly provided by Professor Gang HU, Nanjing Medical University, China. The AQP4-KO mice were

generated as previously described^[29], housed at a controlled temperature (22 ± 1°C) under a 12-h light/dark cycle, and allowed free access to food and water. All experiments were approved by the Institutional Animal Care and Use Committee of Zhejiang University School of Medicine.

2.2 Identification of AQP4 deficiency AQP4 expression was determined by reverse transcription-polymerase chain reaction (RT-PCR) and immunohistochemistry. Total RNA extraction and cDNA synthesis were performed as reported previously^[30,31]. PCR was done on an Eppendorf Mastercycler as follows: 1 µL cDNA mixture was reacted in 20 µL reaction buffer containing 1.5 mmol/L MgCl₂, 0.2 mmol/L dNTPs, 20 pmol/L primer, and 1 U Taq DNA polymerase. The reactions were initially heated at 94°C for 1 min; then at 94°C for 60 s, 60°C for 60 s and 72°C for 60 s, for a total of 35 cycles; and stopped at 72°C for 10 min. PCR products of 10 µL were separated by 2% agarose gel electrophoresis and visualized by ethidium bromide staining. The primer sequences were as follows: AQP4, forward 5'-CTGGAGCCAGCATGAATCCAG-3' and reverse 5'-TTCTTCTCTTCTCCACGGTCA-3'; β-actin, forward 5'-AACCTAAGGCCAACCGTGAA-3' and reverse 5'-TCATGAGGTAGTCTGTTCAGGTC-3'. The product sizes were 270 bp and 450 bp, respectively. Immunohistochemical staining for AQP4 was performed using a rabbit anti-AQP4 polyclonal antibody (1:150; Chemicon International, Temecula, CA) as reported previously^[32].

Water intoxication was evaluated to determine the deficiency of AQP4 function. The mice were anesthetized by intraperitoneal injection of chloral hydrate (400 mg/kg), then intraperitoneally injected with 0.4 µg/kg 1-desamino-8-d-arginine vasopressin (DDAVP), followed 30 min later by distilled water injection of 20% of the body weight. The death rate was recorded at 10-min intervals within the initial 90 min and thereafter at 2-h intervals within 24 h^[33].

2.3 Focal cerebral ischemia The mice were anesthetized by intraperitoneal injection of chloral hydrate (400 mg/kg). A polyethylene catheter was inserted into the right femoral artery for continuous monitoring of blood pressure using a computer-assisted system (PC-Lab, Kelong Inc., Nanjing, China), and for measuring *p*O₂, *p*CO₂, and arterial

pH (Blood Gas Analyzer ABL 330, Leidu Inc., Denmark). Blood glucose was monitored by a one-touch basic blood glucose monitoring system (Lifescan Inc., USA). Rectal temperature was measured and maintained at $37.0 \pm 0.5^\circ\text{C}$ with a heating pad and a heating lamp during surgery.

Focal cerebral ischemia was induced by middle cerebral artery occlusion (MCAO) as described previously^[34], based on modifications of a rat model originally described by Longa *et al.*^[35]. Briefly, a 6-0 nylon monofilament suture, blunted at the tip and coated with 1% poly-*L*-lysine, was inserted into the internal carotid artery, and advanced approximately 10 mm distal to the carotid bifurcation to occlude the origin of the middle cerebral artery. Thirty minutes after occlusion, the suture was withdrawn to allow reperfusion. In sham-operated animals, the same procedure was done with the exception of inserting the intraluminal filament. After surgery, mice were kept for about 2 h in a warm box heated by lamps to maintain body temperature.

2.4 Histopathological and immunohistochemical examination The brain was removed, fixed in 4% paraformaldehyde overnight, and transferred to 30% sucrose for 3–5 days. Sequential 10- μm coronal sections were cut on a cryomicrotome (CM1900, Leica, Wetzlar, Germany) for pathological or immunohistochemical examination. For histopathological examination, the sections were stained with 1% toluidine blue, and surviving neurons (large cells with a pyramidal appearance without being shrunken) were counted in the ischemic core and boundary zone, in five 200- μm^2 squares for each zone. The investigators were blinded to the genotypes of mice when they measured neuron numbers.

For immunohistochemical examination, the sections were blocked with 0.3% H_2O_2 in methanol for 30 min, hydrated gradually to distilled water, and incubated for 2 h with 5% goat serum to block nonspecific immune reactions. Sections were then incubated overnight at 4°C with rabbit polyclonal antibodies against ionized calcium-binding adaptor molecule 1 (Iba-1, a marker of microglia, 1:1 000; Wako, Osaka, Japan), glial fibrillary acidic protein (GFAP, a marker of astrocytes, 1:600; Chemicon, Billerica, MA) and myeloperoxidase (MPO, a marker of neutrophilic

granulocytes, 1:800; R&D Systems, Minneapolis, MN). After washing, the sections were incubated with biotinylated goat anti-rabbit IgG (1:200) for 2 h, followed by incubation with avidin-biotin-peroxidase complex (1:200) for 2 h. Finally, the sections were exposed for 0.5–2 min to 0.01% 3, 3'-diaminobenzidine. The stained sections were examined under a light microscope (Olympus BX51, Tokyo, Japan), and Iba-1-positive, GFAP-positive and MPO-positive cells were counted in five 200- μm^2 squares in the temporoparietal cortical layers III and IV in the ischemic core, boundary zone, and at the same location in the contralateral uninjured cortex. No positive staining was detected when normal goat serum was used instead of the primary antibody.

For double immunofluorescence staining, the 10- μm frozen sections were blocked with 5% normal goat serum or donkey serum for nonspecific binding of IgG for 2 h at room temperature, then double-labeled with the rabbit polyclonal anti-CysLT₁ (1:1 000) or anti-CysLT₂ receptor antibody (1:1 000), and with one of the following antibodies: a mouse monoclonal anti-NeuN antibody (1:200), anti-GFAP (1:600), anti-MPO (1:800), or goat polyclonal anti-Iba1 antibody (1:400) in 10 mmol/L PBS containing 0.1% TritonX-100 overnight at 4°C . Goat anti-rabbit FITC, goat anti-rabbit Cy3, goat anti-mouse FITC, donkey anti-rabbit Cy3, and donkey anti-goat FITC (all 1:200, Chemicon) were used as secondary antibodies for 2 h at room temperature. The stained sections were examined under a fluorescence microscope (Olympus BX51).

2.5 Western blotting analysis At 24 h and 72 h after MCAO, cortical tissues were obtained from the ischemic and contralateral hemispheres, and homogenized in immunoprecipitation assay buffer, pH 7.5, containing (in mmol/L) pepstatin 1, leupeptin 2, phenylmethyl-sulfonyl fluoride 1, and aprotinin 80 (Kangcheng Biotechnology Inc., Shanghai, China). The homogenate was centrifuged at 12 000 g for 30 min at 4°C . The protein samples (30 μg) were loaded on 10% SDS-PAGE and blotted onto nitrocellulose membranes (Invitrogen). The membranes were then incubated overnight with the rabbit polyclonal anti-CysLT₁ or -CysLT₂ receptor antibody (1:200) that were prepared in our laboratory as reported previously^[36,37], or with mouse

monoclonal anti-GAPDH antibody (1:6 000, Kangcheng Biotechnology Inc.). The membranes were then incubated with anti-rabbit IRDye700DX-conjugated antibody or anti-mouse IRDye800DX-conjugated antibody (1:4 000, Rockland, Gibertsville, PA). Specific signals were detected by an Odyssey infrared imaging system (LI-COR Biosciences, Lincoln, NE). The protein bands were quantitatively evaluated by densitometry using Quantity One analysis software (Bio-Rad Laboratories, Hercules, CA).

2.6 Statistical analysis Data are expressed as mean \pm SEM. Statistical analyses were performed using one-way analysis of variance followed by Newman-Keuls *post hoc* multiple comparison using SPSS 11.5 for windows. $P < 0.05$ was considered statistically significant.

3 Results

3.1 Identification of AQP4 deficiency

AQP4 mRNA (Fig. 1A) and AQP4-positive cells (Fig. 1B) were detectable in wild-type mice but not in AQP4-KO mice. The results of water intoxication showed that the survival of AQP4-KO mice was higher than wild-type mice (100% vs 58.3% at 60 min; 91.7% vs 50% at 90 min) (Fig. 1C), which is consistent with a previous report^[33]. These results confirmed the deficiency of the AQP4 gene in AQP4-KO mice.

3.2 Cellular responses in the brain after MCAO No significant difference was found in mean arterial blood pressure, pO_2 , pCO_2 , arterial pH and glucose between 30 min before and 30 min after MCAO. There was no difference in these variables between wild-type and AQP4-KO mice (Table 1).

At 24 h and 72 h after MCAO, the number of apparently surviving neurons with intact morphology was reduced in both the ischemic core and boundary zone. In the ischemic core more neurons were lost than in the boundary

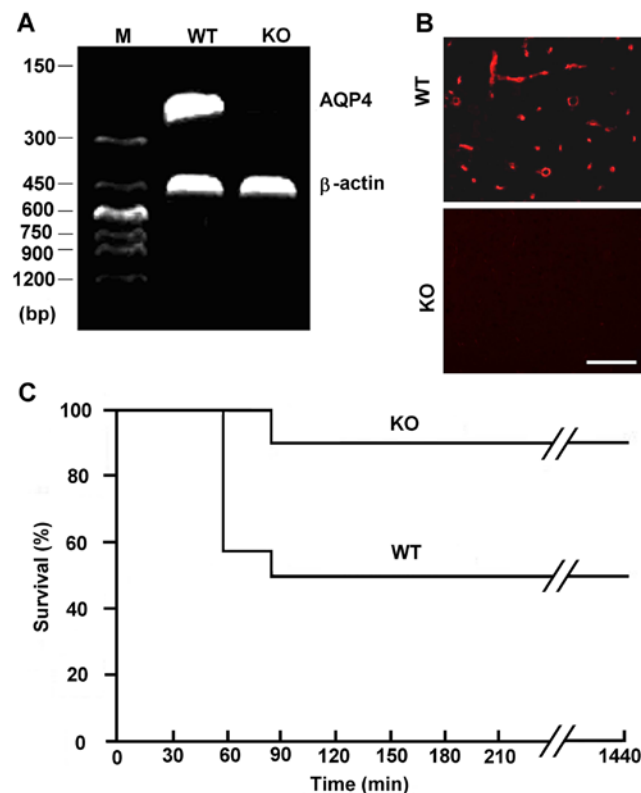


Fig. 1. Identification of AQP4 deficiency. A and B: Brain tissue from AQP4-knockout (KO) mice did not express AQP4 mRNA (A) and protein (B). Scale bar, 25 μ m. C: After water intoxication induced by intraperitoneal injection of distilled water (20% body weight) containing DDAVP (0.4 μ g/kg), the survival rate at 24 h (1440 min) was higher in AQP4-KO mice than in wild-type mice. $P < 0.05$ analyzed by χ^2 test; $n = 10$ –12 mice per group.

Table 1. Summary of physiological variables before and after operation

Variables		Sham operation (<i>n</i> = 8)	MCAO	
			Wide-type (<i>n</i> = 8)	AQP4-knockout (<i>n</i> = 8)
MABP (mmHg)	30 min before MCAO	86.7 ± 5.4	85.9 ± 3.9	85.8 ± 4.2
	30 min after MCAO	85.0 ± 5.7	88.3 ± 4.8	84.0 ± 5.0
<i>p</i> O ₂ (mmHg)	30 min before MCAO	124 ± 5	125 ± 3	123 ± 4
	30 min after MCAO	125 ± 2	122 ± 5	121 ± 6
<i>p</i> CO ₂ (mmHg)	30 min before MCAO	37.2 ± 1.0	36.4 ± 1.1	35.8 ± 1.7
	30 min after MCAO	39.0 ± 1.9	38.1 ± 1.7	37.3 ± 2.0
Glucose (mmol/L)	30 min before MCAO	6.43 ± 0.90	5.97 ± 0.69	6.26 ± 0.67
	30 min after MCAO	5.89 ± 0.93	5.67 ± 0.80	5.94 ± 0.56
pH	30 min before MCAO	7.34 ± 0.02	7.35 ± 0.04	7.35 ± 0.02
	30 min after MCAO	7.34 ± 0.03	7.34 ± 0.05	7.36 ± 0.03

AQP4, aquaporin-4; MABP, mean arterial blood pressure; MCAO, middle cerebral arterial occlusion.

zone, and no surviving neurons were detectable at 72 h (Fig. 2A). Besides, AQP4-KO mice lost more neurons than

wild-type mice at 24 h and 72 h in the boundary zone; while no difference was found in the ischemic core (Fig. 2B).

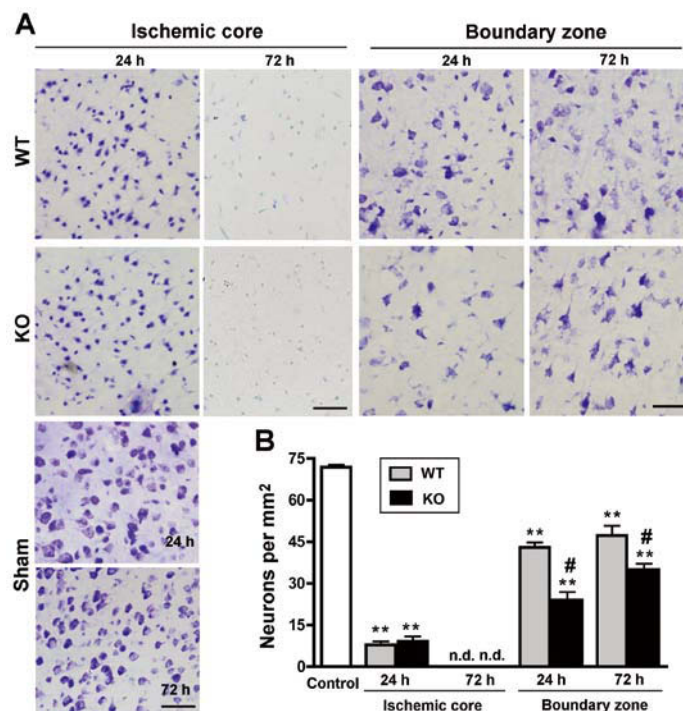


Fig. 2. Neuron density after MCAO in wild-type (WT) and AQP4-knockout (KO) mice. **A:** Photomicrographs from ischemic hemispheres showing neurons stained with 1% toluidine blue at 24 and 72 h after MCAO. Scale bars, 50 μ m. **B:** Summarized data showing more neuronal loss in the boundary zone in AQP-KO mice than in wild-type mice. Mean \pm SEM; *n* = 8; ***P* < 0.01 compared with sham-operated mice, #*P* < 0.05 compared with wild-type mice, analyzed by one-way ANOVA.

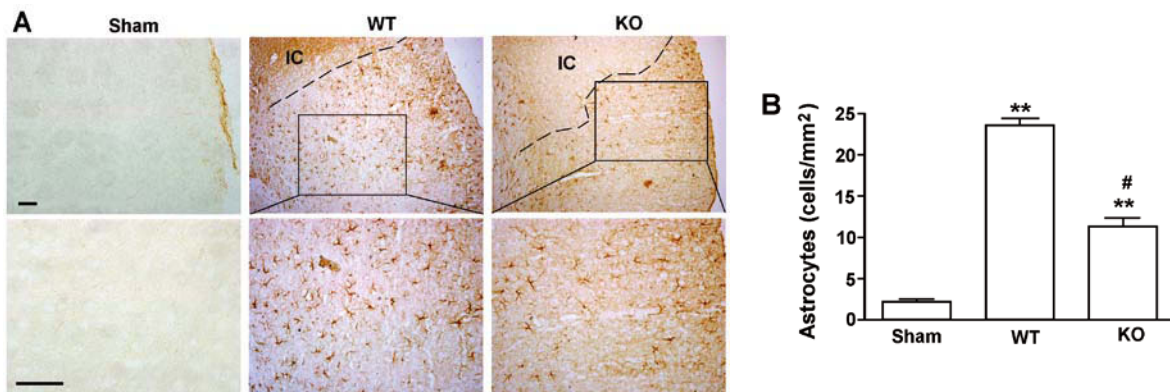


Fig. 3. Astrocyte response in the boundary zone after MCAO in wild-type (WT) and AQP4-knockout (KO) mice. **A:** Photomicrographs from ischemic hemispheres showing marked increases in GFAP immuno-positive astrocytes in the boundary zone 72 h after MCAO. Lower panels show zoomed areas in the upper. Scale bars, 50 μ m (upper panels) and 25 μ m (lower panels). IC, ischemic core. **B:** Relative optical density of GFAP immunostaining presented in A. Summarized data show that the increase in astrocyte number was less pronounced in AQP4-KO mice than in ischemic wild-type mice. Mean \pm SEM; $n = 8$; ** $P < 0.01$ compared with sham-operated mice, # $P < 0.05$ compared with wild-type mice, analyzed by one-way ANOVA.

Immunostaining with anti-GFAP antibody showed that the number of astrocytes in both the ischemic core and boundary zone did not change 24 h after MCAO (data not shown). Astrocytes were not detectable in the ischemic core, but increased in the boundary zone 72 h after MCAO (Fig. 3A). The increase in astrocytes compared to the sham-operated mice was significantly less in AQP4-KO mice than in wild-type mice (Fig. 3B).

Immunostaining with anti-Iba-1 antibody showed that Iba-1-positive microglia did not substantially change in the ischemic core 24 h and 72 h after MCAO (data not shown). However, the number of microglia increased in the boundary zone at 24 h and 72 h. The increased microglia at 72 h showed two types of morphology. Those in the inner periphery were hypertrophic and amoeboid, i.e. exhibited an activated morphology (Fig. 4A-b), while those in the distant periphery were ramified, which corresponds to a relatively resting state (Fig. 4A-c). In the boundary zone, the microglia were ramified at 24 h, and their density was not significantly different between wild-type and AQP4-KO mice (Fig. 4B). At 72 h, however, the ramified microglia were significantly fewer but the numbers of activated microglia were higher in AQP4-KO mice than in wild-type mice (Fig. 4B, C).

The number of MPO-positive neutrophils increased

in the ischemic core 24 h and 72 h after MCAO (Fig. 5A). The cell density was significantly higher in AQP4-KO mice than in wild-type mice (Fig. 5B). Taken together, these findings indicated that AQP4 KO aggravated the responses of inflammatory cells but attenuated the astrocyte response in addition to aggravating neuronal loss in the ischemic brain.

3.3 Expression and localization of CysLT₁ and CysLT₂ receptors To determine the expression and cellular localization of CysLT₁ and CysLT₂ receptors in the ischemic brain, we performed Western blotting analysis and double immunofluorescence staining. Western blotting analysis showed that CysLT₁ receptor expression was significantly up-regulated at 72 h, while the CysLT₂ receptor was up-regulated mildly at 24 h and greatly at 72 h after MCAO. The expression of both receptors at 72 h was higher in AQP4-KO mice than in wild-type mice (Fig. 6). The expression in AQP4-KO mice increased 156% and 71% more than in wild-type mice: CysLT₁ receptor (ratio to GAPDH), 1.46 ± 0.32 vs 0.57 ± 0.02 ($n = 6$, $P < 0.05$, t -test); CysLT₂ receptor, 2.07 ± 0.22 vs 1.21 ± 0.12 ($n = 6$, $P < 0.01$, t -test).

Based on the spatiotemporal properties of the cellular responses to ischemia and reported findings^[26,30], we performed double immunofluorescence staining to detect the localization of CysLT₁ and CysLT₂ receptors in the

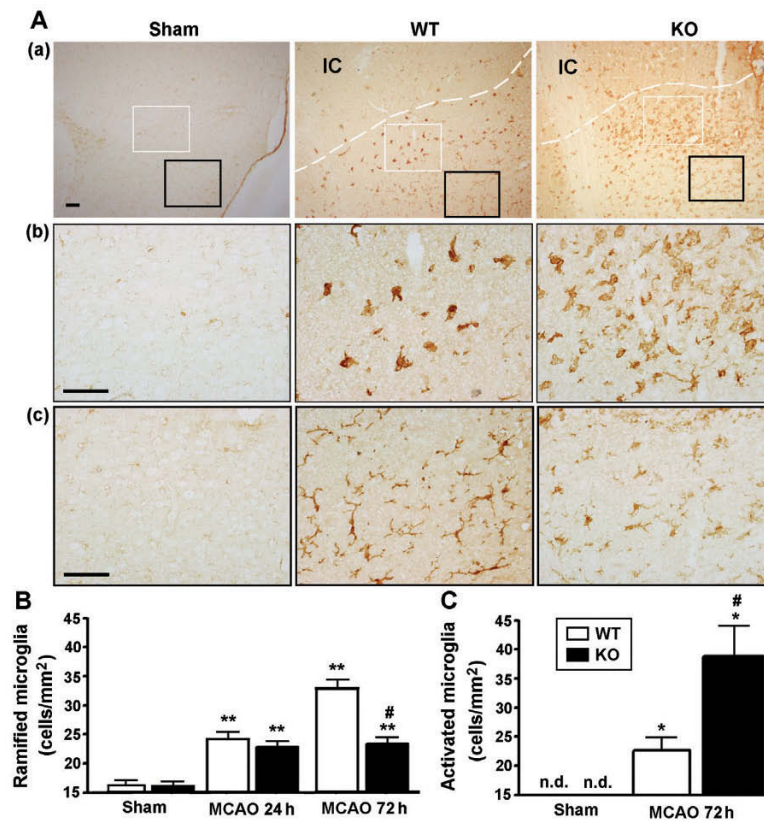


Fig. 4. Microglial activation in the boundary zone after MCAO in wild-type (WT) and AQP4-knockout (KO) mice. **A:** Photomicrographs showing clearly increased Iba-1 immunoreactivity in the boundary zone 72 h after MCAO. The microglia in the inner boundary (close to the ischemic core) showed an activated (hypertrophic and amoeboid) morphology [white square in (a), and (b)]; however, those in distant areas showed a ramified morphology [black square in (a), and (c)]. Microglia were relatively fewer in the ischemic core than in the boundary zone. IC, ischemic core. Scale bars, 50 μ m (a) and 25 μ m (b and c). **B:** Summary data showing increased numbers of ramified microglia in the distant boundary 24 and 72 h after MCAO, and the increase at 72 h was less in AQP4-KO mice than in wild-type mice. **C:** Activated microglia in the inner boundary increased, and the increase was much greater in AQP4-KO mice than in wild-type mice. Mean \pm SEM, $n = 10$; * $P < 0.05$ and ** $P < 0.01$ compared with sham-operated mice, # $P < 0.05$ compared with wild-type mice, analyzed by one-way ANOVA.

ischemic core at 24 h, and in the boundary zone at 72 h after MCAO. In the normal brain from sham-operated mice, CysLT₁ receptor immunoreactivity was not found in NeuN-positive neurons, GFAP-positive astrocytes or Iba-1-positive microglia; and no MPO-positive neutrophils were detectable (data not shown). In the ischemic core at 24 h, the expression of CysLT₁ receptors was increased. The CysLT₁ receptors were mainly localized in neurons and neutrophils, and no immunoreactivity was found in astrocytes and microglia (Fig. 7). In the boundary zone at 72 h, CysLT₁ receptor was also found in most neurons, and in a few astrocytes and microglia. In AQP4-KO mice, the CysLT₁ receptor immunoreactivity was enhanced in neurons

and neutrophils at 24 h in the ischemic core as well as in microglia at 72 h in the boundary zone compared to wild-type mice. The number of astrocytes at 72 h in the boundary zone was markedly reduced and they did not express the CysLT₁ receptor in AQP4-KO mice (Fig. 7).

The localization pattern of CysLT₂ receptors was similar to that of CysLT₁; it was absent from the normal brain, increased in the ischemic core and mainly localized in neurons and neutrophils 24 h after MCAO. At 72 h, the CysLT₂ receptors were mainly localized in neurons and some in astrocytes and microglia in the boundary zone; however, the localization in microglia was markedly enhanced in AQP4-KO mice (Fig. 8).

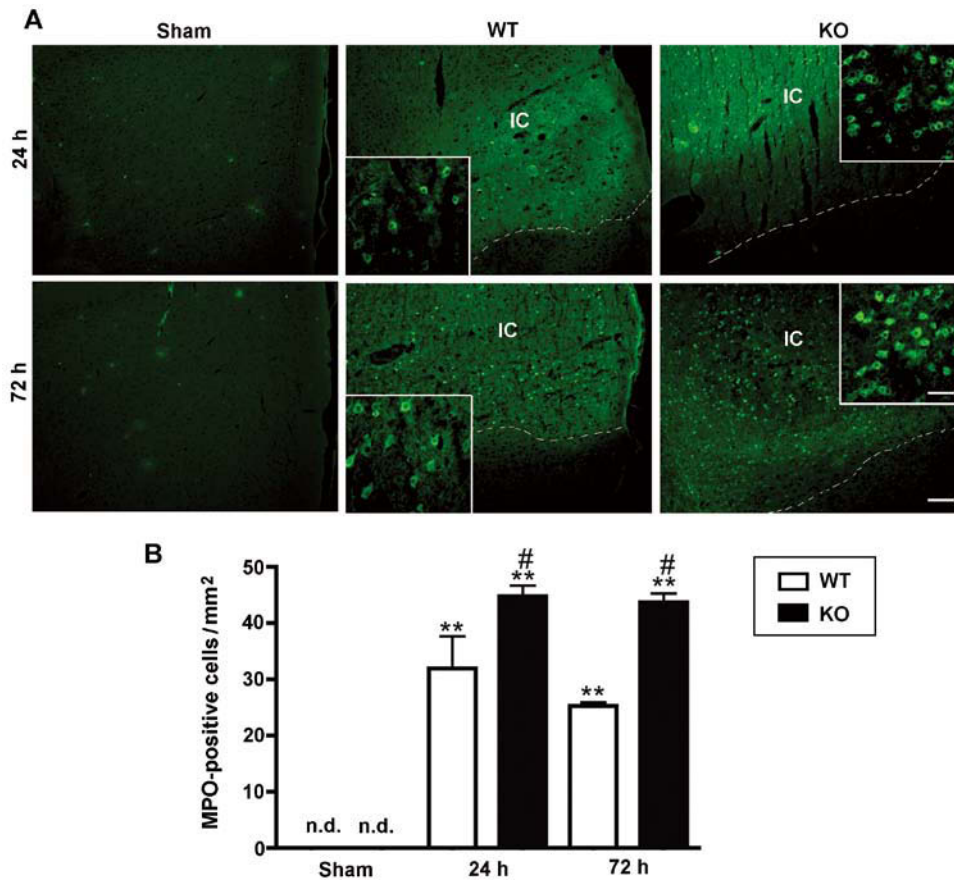


Fig. 5. MPO-positive cells after MCAO in wild-type (WT) and AQP4-knockout (KO) mice. A: Photomicrographs showing clear increases in MPO-positive cells in the ischemic core 24 and 72 h after MCAO. IC, ischemic core. Scale bars, 50 μ m and 25 μ m (in the insert). B: Summary of data for MPO-positive cells. Mean \pm SEM; $n = 8$; ** $P < 0.01$ compared with sham operation, # $P < 0.05$ compared with wild-type mice, analyzed by one-way ANOVA.

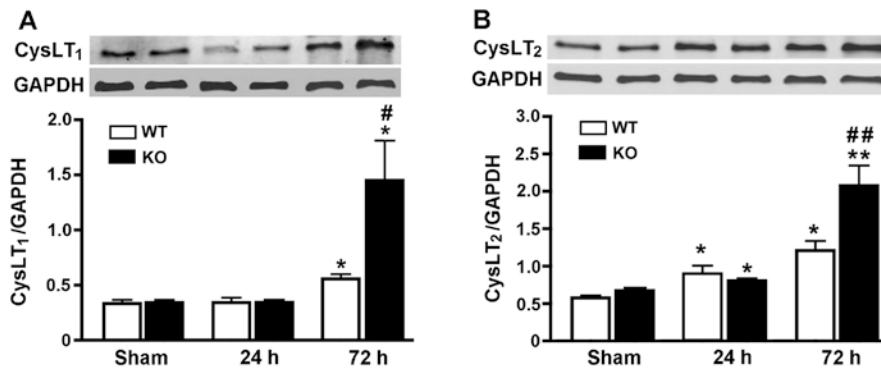


Fig. 6. Expression of CysLT₁ and CysLT₂ receptors in brain after MCAO in wild-type (WT) and AQP4-knockout (KO) mice. A: Western blotting analysis showed that expression of the CysLT₁ receptors was significantly up-regulated 72 h after MCAO; and the expression was higher in AQP4-KO mice than in wild-type mice. B: CysLT₂ receptor expression was up-regulated 24 and 72 h after MCAO; and the expression at 72 h was higher in AQP4-KO mice than in wild-type mice. Mean \pm SEM; $n = 8$; * $P < 0.05$ and ** $P < 0.01$ compared with sham-operated mice, # $P < 0.05$ and ## $P < 0.01$ compared with wild-type mice (t test).

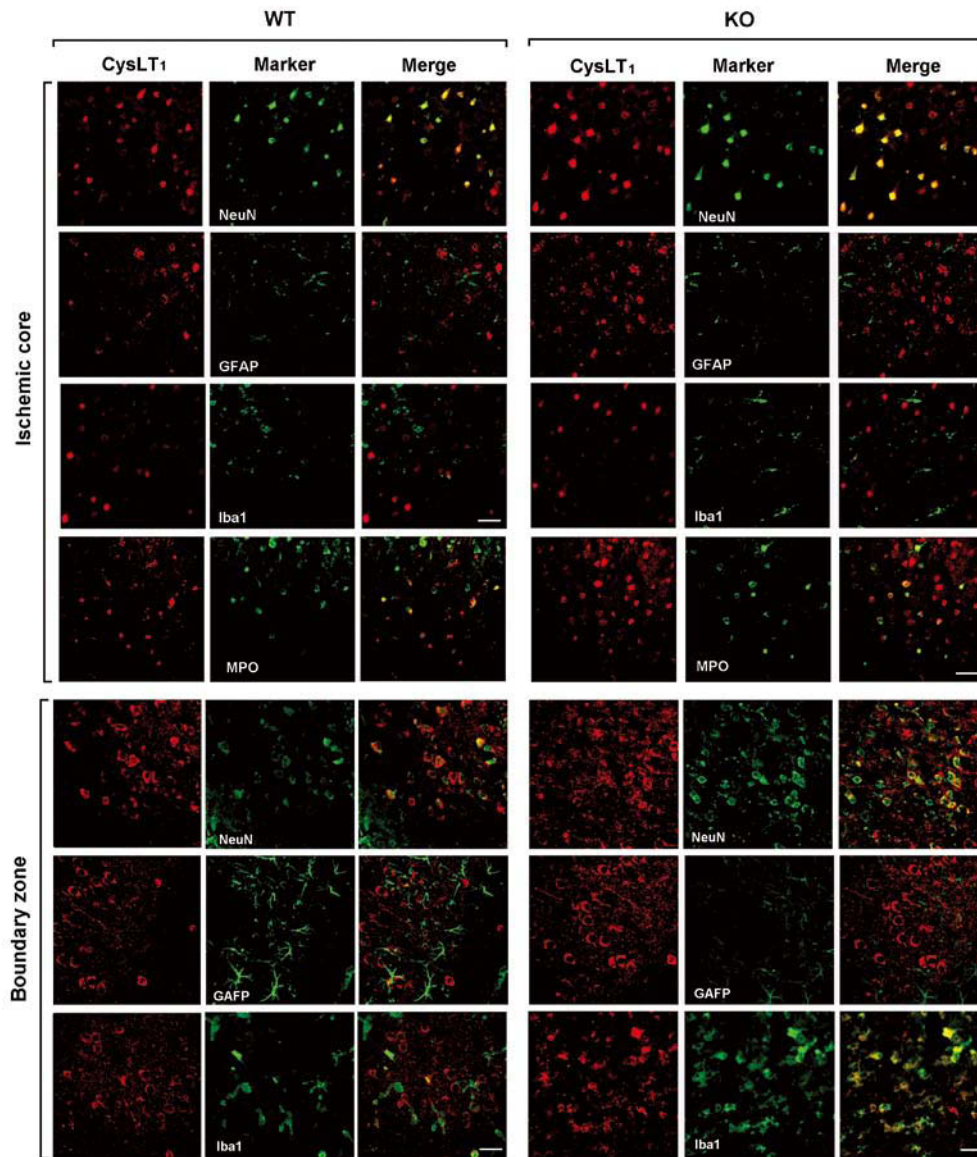


Fig. 7. CysLT₁ receptor localization in brain after MCAO. In the ischemic core, CysLT₁ receptor immunoreactivity clearly increased and was localized in NeuN-positive neurons and MPO-positive neutrophils, but not in GFAP-positive astrocytes or Iba-1-positive microglia 24 h after MCAO. In the boundary zone, it was mainly localized in neurons but in a few astrocytes and microglia 72 h after MCAO. The co-localization in microglia was stronger in AQP4-knockout (KO) mice than in wild-type (WT) mice. Scale bars, 50 μm. Experiments were repeated 3–4 times with similar results.

We also found that, in the ischemic core 72 h after MCAO, neurons and astrocytes disappeared; the number of microglia was mildly increased but they did not express CysLT₁ and CysLT₂ receptors. The number of neutrophils was remarkably increased, and they expressed both receptors in AQP4-KO and wild-type mice (data not shown).

4 Discussion

The results of the present study suggest that AQP4 may play an inhibitory role in post-ischemic inflammation. The evidence is that AQP4-KO mice exhibited more severe cellular inflammation after MCAO, including neutrophil infiltration in the ischemic core and microglial activation

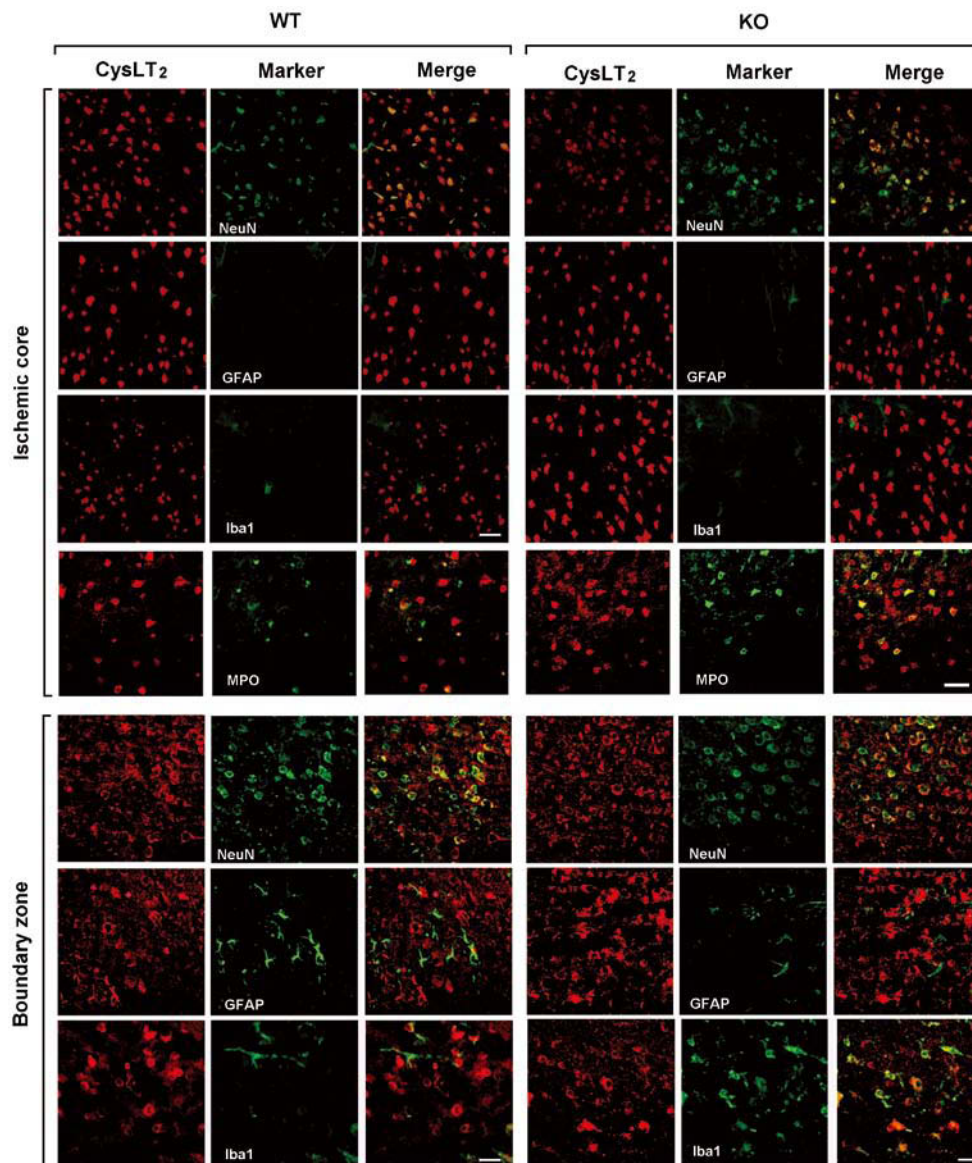


Fig. 8. CysLT₂ receptor localization in brain after MCAO. In the ischemic core, CysLT₂ receptor immunoreactivity clearly increased and was localized in NeuN-positive neurons and MPO-positive neutrophils 24 h after MCAO, but not in GFAP-positive astrocytes and Iba-1-positive microglia 72 h after MCAO. In the boundary zone, it was mainly localized in neurons but in a few astrocytes and microglia 72 h after MCAO. The co-localization in microglia was stronger in AQP4-KO mice than in wild-type mice. Scale bars, 50 μ m. Experiments were repeated 3–4 times with similar results.

in the boundary zone, but the proliferation of astrocytes was attenuated. Moreover, the up-regulated expression of the inflammation-related receptors CysLT₁ and CysLT₂ and their localization in injured neurons, infiltrating neutrophils and activated microglia were enhanced in AQP4-KO mice.

We found that astrocyte proliferation in the boundary zone 72 h after MCAO was attenuated in AQP4-KO mice;

such an inhibition could also be induced by knockdown of AQP4 using siRNA *in vitro*^[19]. The attenuated astrocyte responses might be related to aggravated cellular inflammation in AQP4-KO mice. Supporting this notion, astrocyte dysfunction induced by NMO-IgG accelerates the development of inflammation^[12]. Moreover, either ablation or attenuation of glial scar-forming astrocytes exacerbates

the spread of inflammatory cells during locally-initiated inflammatory responses to brain trauma or spinal cord injury^[38–41], or during peripherally-initiated experimental autoimmune encephalomyelitis^[18,42]. As another possibility, the numbers of CD4⁺ CD25⁺ regulatory T cells are reduced in AQP4-KO mice^[43], suggesting that AQP4 KO disrupts immunosuppressive regulators, thereby resulting in hyperactive immune and inflammatory responses.

The aggravated cellular inflammation might, in turn, be one of the factors that induce more severe neuronal injury after MCAO in AQP4-KO mice, because inflammatory cells, both activated microglia and infiltrating neutrophils, express and release pro-inflammatory mediators such as the toxic cytokines IL-1 and TNF- α ^[44,45]. Reduction of glutamate uptake and the expression of the excitatory amino-acid transporter GLT-1 in astrocytes of AQP4-KO mice^[46] might also worsen the neuronal injury by potentiating excitatory toxicity in the acute phase of ischemia.

Another important finding is that AQP4-KO mice had a more pronounced up-regulation of CysLT₁ and CysLT₂ receptor expression at 72 h after MCAO compared with wild-type mice. This temporal pattern of expression matched the enhanced inflammatory responses at this time point in AQP4-KO mice. Both CysLT₁ and CysLT₂ receptors were primarily localized in neurons and neutrophils in the ischemic core; and their expression in microglia in the boundary zone was enhanced in AQP4-KO mice. Similar expression and localization properties of these receptors have been reported in rat brain after MCAO^[26,30]. However, in the present study we focused on the delayed phase (72 h) to reveal the inflammatory responses in AQP4-KO mice. The spatiotemporal patterns imply that the enhanced CysLT₁ and CysLT₂ receptors in AQP4-KO mice might be associated with aggravation of post-ischemic neuronal injury and inflammatory responses. Why AQP4-KO mice exhibited an enhanced up-regulation of CysLT₁ and CysLT₂ receptors cannot be explained in the present study. However, one of the possibilities is that the enhanced inflammatory responses due to astrocyte dysfunction may, *via* a series of events, secondarily potentiate inflammation-related molecules in AQP4-KO mice^[12,16,17]; the up-regulation of CysLT₁ and

CysLT₂ receptors (Figs. 6–8) might be induced in such a way. These up-regulated receptors might, in turn, enhance the inflammatory responses in AQP4-KO mice. Of course, since a complex of post-ischemic events is involved in the inflammatory responses, other pro-inflammatory mediators such as cytokines, chemokines, oxygen and nitrogen free radicals and matrix metalloproteinases^[47] may also respond to aggravated inflammation in AQP4-KO mice.

Our findings suggest that AQP4 KO may aggravate ischemic insults, i.e. more severe cellular inflammation and neuronal injury, and profoundly up-regulated CysLT₁ and CysLT₂ receptors. In other words, AQP4 may be a suppressing or protective regulator of post-ischemic inflammation. The protective role of AQP4 in ischemic brain injury is also reported elsewhere. For example, the early induction of AQP4 by a low dose of thrombin contributes to limitation of the ischemic infarction and formation of edema in mice^[48], and acute vascular disruption is associated with AQP4 loss after transient MCAO in rats^[49]. This protective role is also reported in spinal cord compression injury^[50], subarachnoid hemorrhage^[51], intracerebral hemorrhage^[52] and 1-methyl-4-phenyl-1,2,3,6-tetrahydropyridine toxicity^[53,54]. These findings demonstrate that AQP4 in astrocytes exerts a beneficial action in pathological conditions. However, AQP4 has also been reported to exert an injurious action in an early phase of brain ischemia, as AQP4 deficiency attenuates cytotoxic edema and the resultant ischemic insult after permanent focal cerebral ischemia^[1,33]. This different finding might be due to different ischemic models and observed indicators, and in the present study we focused on cellular and molecular inflammatory responses at 24 h and 72 h after transient focal cerebral ischemia in AQP4-KO mice. Because post-ischemic responses are highly complex, the role of AQP4 in post-ischemic inflammation and repair processes in the delayed or chronic phases needs further investigation.

In conclusion, we found that AQP4-KO mice exhibited more severe cellular inflammation and enhanced expression of the inflammation-related CysLT₁ and CysLT₂ receptors after MCAO, suggesting that AQP4 may play an inhibitory role in post-ischemic inflammation.

Acknowledgements: This work was supported by the National Natural Science Foundation of China (81273491, 81072618, 30772561 and 30873053), the Natural Science Foundation of Zhejiang Province, China (Y2090069), the “Qianjiang Rencai Research Plan” of Zhejiang Province China (2010R10055), and the Fundamental Research Funds for the Central Universities, China (2009QNA7008). We thank Prof. G Hu, Nanjing Medical University, China, for providing AQP4-knockout mice.

References:

- [1] Papadopoulos MC, Verkman AS. Aquaporin-4 and brain edema. *Pediatr Nephrol* 2007, 22: 778–784.
- [2] Saadoun S, Papadopoulos MC. Aquaporin-4 in brain and spinal cord oedema. *Neuroscience* 2010, 168: 1036–1046.
- [3] Satoh J, Tabunoki H, Yamamura T, Arima K, Konno H. Human astrocytes express aquaporin-1 and aquaporin-4 *in vitro* and *in vivo*. *Neuropathology* 2007, 27: 245–256.
- [4] Auguste KI, Jin S, Uchida K, Yan D, Manley GT, Papadopoulos MC, *et al.* Greatly impaired migration of implanted aquaporin-4-deficient astroglial cells in mouse brain toward a site of injury. *FASEB J* 2007, 21: 108–116.
- [5] Saadoun S, Papadopoulos MC, Watanabe H, Yan D, Manley GT, Verkman AS. Involvement of aquaporin-4 in astroglial cell migration and glial scar formation. *J Cell Sci* 2005, 118: 5691–5698.
- [6] Thrane AS, Rappold PM, Fujita T, Torres A, Bekar LK, Takano T, *et al.* Critical role of aquaporin-4 (AQP4) in astrocytic Ca^{2+} signaling events elicited by cerebral edema. *Proc Natl Acad Sci U S A* 2011, 108: 846–851.
- [7] Ding JH, Sha LL, Chang J, Zhou XQ, Fan Y, Hu G. Alterations of striatal neurotransmitter release in aquaporin-4 deficient mice: An *in vivo* microdialysis study. *Neurosci Lett* 2007, 422: 175–180.
- [8] Aoki-Yoshino K, Uchihara T, Duyckaerts C, Nakamura A, Hauw JJ, Wakayama Y. Enhanced expression of aquaporin 4 in human brain with inflammatory diseases. *Acta Neuropathol* 2005, 110: 281–288.
- [9] Huang XN, Wang WZ, Fu J, Wang HB. The relationship between aquaporin-4 expression and blood-brain and spinal cord barrier permeability following experimental autoimmune encephalomyelitis in the rat. *Anat Rec (Hoboken)* 2011, 294: 46–54.
- [10] Miyamoto K, Nagaosa N, Motoyama M, Kataoka K, Kusunoki S. Upregulation of water channel aquaporin-4 in experimental autoimmune encephalomyelitis. *J Neurol Sci* 2009, 276: 103–107.
- [11] Graber DJ, Levy M, Kerr D, Wade WF. Neuromyelitis optica pathogenesis and aquaporin 4. *J Neuroinflammation* 2008, 5: 22.
- [12] Hinson SR, McKeon A, Lennon VA. Neurological autoimmunity targeting aquaporin-4. *Neuroscience* 2010, 168: 1009–1018.
- [13] Wu H, Zhang Z, Li Y, Zhao R, Li H, Song Y, *et al.* Time course of upregulation of inflammatory mediators in the hemorrhagic brain in rats: correlation with brain edema. *Neurochem Int* 2010, 57: 248–253.
- [14] Sharma R, Fischer MT, Bauer J, Felts PA, Smith KJ, Misu T, *et al.* Inflammation induced by innate immunity in the central nervous system leads to primary astrocyte dysfunction followed by demyelination. *Acta Neuropathol* 2010, 120: 223–236.
- [15] Tourdias T, Mori N, Dragonu I, Cassagno N, Boiziau C, Aussudre J, *et al.* Differential aquaporin 4 expression during edema build-up and resolution phases of brain inflammation. *J Neuroinflammation* 2011, 8: 143.
- [16] Matsushita T, Isobe N, Matsuoka T, Ishizu T, Kawano Y, Yoshiura T, *et al.* Extensive vasogenic edema of anti-aquaporin-4 antibody-related brain lesions. *Mult Scler* 2009, 15: 1113–1117.
- [17] Saikali P, Cayrol R, Vincent T. Anti-aquaporin-4 auto-antibodies orchestrate the pathogenesis in neuromyelitis optica. *Autoimmun Rev* 2009, 9: 132–135.
- [18] Voskuhl RR, Peterson RS, Song B, Ao Y, Morales LB, Tiwari-Woodruff S, *et al.* Reactive astrocytes form scar-like perivascular barriers to leukocytes during adaptive immune inflammation of the CNS. *J Neurosci* 2009, 29: 11511–11522.
- [19] Kuppens E, Gleiser C, Brito V, Wachter B, Pauly T, Hirt B, *et al.* AQP4 expression in striatal primary cultures is regulated by dopamine—implications for proliferation of astrocytes. *Eur J Neurosci* 2008, 28: 2173–2182.
- [20] Kriz J. Inflammation in ischemic brain injury: timing is important. *Crit Rev Neurobiol* 2006, 18: 145–157.
- [21] Wang Q, Tang XN, Yenari MA. The inflammatory response in stroke. *J Neuroimmunol* 2007, 184: 53–68.
- [22] Xia W, Han J, Huang G, Ying W. Inflammation in ischaemic brain injury: current advances and future perspectives. *Clin Exp Pharmacol Physiol* 2010, 37: 253–258.
- [23] Chu LS, Wei EQ, Yu GL, Fang SH, Zhou Y, Wang ML, *et al.* Pranlukast reduces neutrophil but not macrophage/microglial accumulation in brain after focal cerebral ischemia in mice. *Acta Pharmacol Sin* 2006, 27: 282–288.
- [24] Fang SH, Wei EQ, Zhou Y, Wang ML, Zhang WP, Yu GL, *et al.* Increased expression of cysteinyl leukotriene receptor-1 in the brain mediates neuronal damage and astrogliosis after focal cerebral ischemia in rats. *Neuroscience* 2006, 140: 969–979.
- [25] Zhou Y, Wei EQ, Fang SH, Chu LS, Wang ML, Zhang WP, *et al.* Spatio-temporal properties of 5-lipoxygenase expression and activation in the brain after focal cerebral ischemia in rats. *Life Sci* 2006, 79: 1645–1656.
- [26] Zhao CZ, Zhao B, Zhang XY, Huang XQ, Shi WZ, Liu HL, *et al.* Cysteinyl leukotriene receptor 2 is spatiotemporally involved in neuron injury, astrocytosis and microgliosis after focal cerebral

- ischemia in rats. *Neuroscience* 2011, 189: 1–11.
- [27] Yu GL, Wei EQ, Wang ML, Zhang WP, Zhang SH, Weng JQ, *et al.* Pranlukast, a cysteinyl leukotriene receptor-1 antagonist, protects against chronic ischemic brain injury and inhibits the glial scar formation in mice. *Brain Res* 2005, 1053: 116–125.
- [28] Huang XJ, Zhang WP, Li CT, Shi WZ, Fang SH, Lu YB, *et al.* Activation of CysLT receptors induces astrocyte proliferation and death after oxygen-glucose deprivation. *Glia* 2008, 56: 27–37.
- [29] Fan Y, Zhang J, Sun XL, Gao L, Zeng XN, Ding JH, *et al.* Sex- and region-specific alterations of basal amino acid and monoamine metabolism in the brain of aquaporin-4 knockout mice. *J Neurosci Res* 2005, 82: 458–464.
- [30] Fang SH, Zhou Y, Chu LS, Zhang WP, Wang ML, Yu GL, *et al.* Spatio-temporal expression of cysteinyl leukotriene receptor-2 mRNA in rat brain after focal cerebral ischemia. *Neurosci Lett* 2007, 412: 78–83.
- [31] Qi LL, Fang SH, Shi WZ, Huang XQ, Zhang XY, Lu YB, *et al.* CysLT2 receptor-mediated AQP4 up-regulation is involved in ischemic-like injury through activation of ERK and p38 MAPK in rat astrocytes. *Life Sci* 2011, 88: 50–56.
- [32] Wang ML, Huang XJ, Fang SH, Yuan YM, Zhang WP, Lu YB, *et al.* Leukotriene D4 induces brain edema and enhances CysLT2 receptor-mediated aquaporin 4 expression. *Biochem Biophys Res Commun* 2006, 350: 399–404.
- [33] Manley GT, Fujimura M, Ma T, Noshita N, Filiz F, Bollen AW, *et al.* Aquaporin-4 deletion in mice reduces brain edema after acute water intoxication and ischemic stroke. *Nat Med* 2000, 6: 159–163.
- [34] Ye YL, Shi WZ, Zhang WP, Wang ML, Zhou Y, Fang SH, *et al.* Cilostazol, a phosphodiesterase 3 inhibitor, protects mice against acute and late ischemic brain injuries. *Eur J Pharmacol* 2007, 557: 23–31.
- [35] Longa EZ, Weinstein PR, Carlson S, Cummins R. Reversible middle cerebral artery occlusion without craniectomy in rats. *Stroke* 1989, 20: 84–91.
- [36] Luo JY, Zhang Z, Yu SY, Zhao B, Zhao CZ, Wang XX, *et al.* Rote none-induced changes of cysteinyl leukotriene receptor 1 expression in BV2 microglial cells. *J Zhejiang Univ Med Sci* 2011, 40: 131–138.
- [37] Zhang LP, Zhao CZ, Shi WZ, Qi LL, Lu YB, Zhang YM, *et al.* Preparation and identification of polyclonal antibody against cysteinyl leukotriene receptor 2. *J Zhejiang Univ Med Sci* 2009, 38: 591–597.
- [38] Bush TG, Puvanachandra N, Horner CH, Polito A, Ostendorf T, Svendsen CN, *et al.* Leukocyte infiltration, neuronal degeneration, and neurite outgrowth after ablation of scar-forming, reactive astrocytes in adult transgenic mice. *Neuron* 1999, 23: 297–308.
- [39] Faulkner JR, Herrmann JE, Woo MJ, Tansey KE, Doan NB, Sofroniew MV. Reactive astrocytes protect tissue and preserve function after spinal cord injury. *J Neurosci* 2004, 24: 2143–2155.
- [40] Herrmann JE, Imura T, Song B, Qi J, Ao Y, Nguyen TK, *et al.* STAT3 is a critical regulator of astrogliosis and scar formation after spinal cord injury. *J Neurosci* 2008, 28: 7231–7243.
- [41] Okada S, Nakamura M, Katoh H, Miyao T, Shimazaki T, Ishii K, *et al.* Conditional ablation of Stat3 or Socs3 discloses a dual role for reactive astrocytes after spinal cord injury. *Nat Med* 2006, 12: 829–834.
- [42] Liedtke W, Edelmann W, Chiu FC, Kucherlapati R, Raine CS. Experimental autoimmune encephalomyelitis in mice lacking glial fibrillary acidic protein is characterized by a more severe clinical course and an infiltrative central nervous system lesion. *Am J Pathol* 1998, 152: 251–259.
- [43] Chi Y, Fan Y, He L, Liu W, Wen X, Zhou S, *et al.* Novel role of aquaporin-4 in CD4+ CD25+ T regulatory cell development and severity of Parkinson's disease. *Aging Cell* 2011, 10: 368–382.
- [44] Huang J, Upadhyay UM, Tamargo RJ. Inflammation in stroke and focal cerebral ischemia. *Surg Neurol* 2006, 66: 232–245.
- [45] Tuttolomondo A, Di Raimondo D, di Sciacca R, Pinto A, Licata G. Inflammatory cytokines in acute ischemic stroke. *Curr Pharm Des* 2008, 14: 3574–3589.
- [46] Zeng XN, Sun XL, Gao L, Fan Y, Ding JH, Hu G. Aquaporin-4 deficiency down-regulates glutamate uptake and GLT-1 expression in astrocytes. *Mol Cell Neurosci* 2007, 34: 34–39.
- [47] Amantea D, Nappi G, Bernardi G, Bageetta G, Corasaniti MT. Post-ischemic brain damage: pathophysiology and role of inflammatory mediators. *FEBS J* 2009, 276: 13–26.
- [48] Hirt L, Ternon B, Price M, Mastour N, Brunet JF, Badaut J. Protective role of early aquaporin 4 induction against postischemic edema formation. *J Cereb Blood Flow Metab* 2009, 29: 423–433.
- [49] Friedman B, Schachtrup C, Tsai PS, Shih AY, Akassoglou K, Kleinfeld D, *et al.* Acute vascular disruption and aquaporin 4 loss after stroke. *Stroke* 2009, 40: 2182–2190.
- [50] Saadoun S, Bell BA, Verkman AS, Papadopoulos MC. Greatly improved neurological outcome after spinal cord compression injury in AQP4-deficient mice. *Brain* 2008, 131: 1087–1098.
- [51] Tait MJ, Saadoun S, Bell BA, Verkman AS, Papadopoulos MC. Increased brain edema in aqp4-null mice in an experimental model of subarachnoid hemorrhage. *Neuroscience* 2010, 167: 60–67.
- [52] Tang Y, Wu P, Su J, Xiang J, Cai D, Dong Q. Effects of Aquaporin-4 on edema formation following intracerebral hemorrhage. *Exp Neurol* 2010, 223: 485–495.
- [53] Fan Y, Kong H, Shi X, Sun X, Ding J, Wu J, *et al.* Hypersensitivity of aquaporin 4-deficient mice to 1-methyl-4-phenyl-1,2,3,6-tetrahydropyridine and astrocytic modulation. *Neurobiol Aging* 2008, 29: 1226–1236.
- [54] Hao C, Liu W, Luan X, Li Y, Gui H, Peng Y, *et al.* Aquaporin-4 knockout enhances astrocyte toxicity induced by 1-methyl-4-phenylpyridinium ion and lipopolysaccharide via increasing the expression of cytochrome P4502E1. *Toxicol Lett* 2010, 198: 225–231.